CHAPTER V

NON-ISOTHERMAL MELT-CRYSTALLIZATION KINETICS OF SYNDIOTACTIC POLYPROPYLENE COMPOUNDED WITH VARIOUS NUCLEATING AGENTS

ABSTRACT

Non-isothermal melt-crystallization behavior of syndiotactic polypropylene (sPP) compounded with 5 percent by weight (wt.%) of some inorganic fillers [i.e. kaolin, talcum, marl, titanium dioxide (TiO_2), and silicon dioxide (SiO_2)] and 1 wt.% of some organic fillers, which are some sorbital derivatives (i.e. DBS, MDBS, and DMDBS) was investigated and reported for the first time. It was found that the ability for these fillers to nucleate sPP fell in the following sequence: DBS > talcum > MDBS > SiO_2 ~ kaolin ~ DMDBS > marl > TiO_2, with DBS being able to shift the crystallization exotherm by ca. 18°C on average, while TiO_2 being able to shift the crystallization exotherm by only ca. 6°C on average, from that of neat sPP. The Avrami analysis revealed the Avrami exponent for sPP compounds varying between 2.9 and 4.3, with the values for neat sPP varying between 3.1 and 6.8. Lastly, the Ziabicki's crystallizability of sPP compounds was greater than that of neat sPP, suggesting an increase in the crystallization ability of sPP with addition of these fillers.

(**Key-words**: syndiotactic polypropylene; crystallization; nucleation)

1. INTRODUCTION

Syndiotactic polypropylene (sPP) of high regio- and stereo-regularities was successfully synthesized using the metallocene catalyst system by Ewen *et al.* [1], instead of the traditional Ziegler-Natta catalyst system [2]. This led to renewed interests in this polymer [3-8]. Despite some of its interesting properties, such as high ductility and high optical transparency, the syndiotactic form of PP (i.e. sPP) has enjoyed less commercial success than its isotactic counterpart (iPP) [9].

Among a number of drawbacks, the slow crystallization rate of sPP is an important factor limiting commercial utilization of this polymer [10]. Studies related to crystallization process of semi-crystalline polymers are of great importance in polymer processing, because the resulting physical properties of the products are strongly related to the extent of crystallization and the morphology formed. Both quiescent isothermal and non-isothermal melt-crystallization studies revealed that sPP is a slowly crystallizing polymer [10-12]. Addition of nucleating agents may help enhance the crystallization rates by providing more sites for nucleation, hence reducing the cycle time. Nucleating agents are either inorganic or organic in their chemical makeup. Some examples for inorganic nucleating agents are talcum, mica, barium sulfate ($BaSO_4$), and calcium carbonate ($CaCO_3$); whereas, some examples for organic ones are sorbitals and their derivatives.

In the present contribution, a differential scanning calorimeter (DSC) was used to study non-isothermal melt-crystallization of neat sPP and sPP compounded with an inorganic filler [i.e. kaolin, talcum, marl, titanium dioxide (TiO_2), or silicon dioxide (SiO_2)] and an organic one which is a sorbitol derivative (i.e. DBS, MDBS, or DMDBS). The experimental data are analyzed based on Avrami and Ziabicki macrokinetic model.

2. THEORITICAL BACKGROUND

The overall isothermal crystallization kinetics is often analyzed by the Avrami model [13-15], in which the relative crystallinity as a function of time $\theta(t)$ can be expressed in the following form:

$$\theta(t) = 1 - \exp\left[-(K_a t)^{n_a}\right] \in [0,1], \qquad (1)$$

where K_a and n_a are the Avrami crystallization rate constant and the Avrami exponent, respectively. Usually, the Avrami rate constant K_a is written in the form of the composite Avrami rate constant k_a (i.e. $k_a = K_a^n$); however, use of K_a is more preferable since its units are given as an inverse of time. Both K_a and n_a are constants specific to a given crystalline morphology and type of nucleation for a particular crystallization condition [16].

In the study of non-isothermal crystallization using DSC, the energy released during the crystallization process appears to be a function of temperature rather than time. As a result, the relative crystallinity as a function of temperature $\theta(T)$ can be formulated as

$$\theta(T) = \frac{\int_{T_o}^{T} \left(\frac{dHc}{dT}\right) dT}{\Delta Hc}, \qquad (2)$$

where T_o and T represent the onset and an arbitrary temperature, respectively, dH_c is the enthalpy of crystallization released during an infinitesimal temperature range dT, and ΔH_c is the overall enthalpy of crystallization for a specific cooling condition.

To use Equation (1) in the analysis of non-isothermal crystallization data obtained by DSC, it is assumed that the sample experiences the same thermal history as designated by the DSC furnace. This may be realized only when the thermal lag between the sample and the furnace is kept minimal. If this assumption is valid, the relation between the crystallization time t and the sample temperature T can be formulated as

$$t = \frac{T_o - T}{\phi}, \qquad (3)$$

where ϕ is the cooling rate. According to Equation (3), the horizontal temperature axis observed in a DSC thermogram for the non-isothermal crystallization data can be transformed into the time scale.

Instead of describing the crystallization process with complicated mathematical models, Ziabicki [17-19] proposed a first-order kinetic equation as a means to describe the kinetics of polymeric phase transformation:

$$\frac{d\theta(t)}{dt} = K(T)[1 - \theta(t)], \qquad (4)$$

where $\theta(t)$ is the relative crystallinity as a function of time and $K(T)$ is a temperature-dependent crystallization rate function. In the case of non-isothermal crystallization, $K(T)$ and $\theta(t)$ functions vary and are dependent on the cooling rate used.

For a given cooling condition, Ziabicki [17-19] showed that the crystallization rate function $K(T)$ can be described by a Gaussian function of the following form:

$$K(T) = K_{max} \exp\left[-4 \ln 2 \frac{(T_c - T_{max})^2}{D^2} \right], \quad (5)$$

where T_{max} is the temperature at which the crystallization rate is maximum, K_{max} is the crystallization rate at T_{max}, and D is the width at half-height of the crystallization rate-temperature function. With use of the isokinetic approximation, integration of Equation (5) over the whole crystallizable range of temperatures ($T_g < T < T_m^0$), for a given cooling condition, leads to an important characteristic value for the crystallization ability G of a semi-crystalline polymer, which is defined as

$$G = \int_{T_g}^{T_m^0} K(T) \mathrm{d}T \approx 1.064 K_{max} D . \quad (6)$$

According to an approximate theory [17], the kinetic crystallizability G characterizes the degree of crystallinity obtained when the polymer is cooled at unit cooling rate from the melting temperature to the glass transition temperature [19].

In case of non-isothermal crystallization studies using DSC where cooling rate is a variable, Equation (6) can be applied when the crystallization rate function $K(T)$ is replaced with a derivative function of the relative crystallinity $\dot{\theta}_\phi(T)$ for a particular cooling rate. Therefore, Equation (6) is replaced by

$$G_\phi = \int_{T_g}^{T_m^0} \dot{\theta}_\phi(T) \mathrm{d}T \approx 1.064 \dot{\theta}_{max,\phi} D_\phi , \quad (7)$$

where $\dot{\theta}_{max,\phi}$ and D_ϕ are the maximum crystallization rate and the width at half-height of the derivative relative crystallinity as a function of temperature $\dot{\theta}_\phi(T)$. According to Equation (7), G_ϕ is the kinetic crystallizability at an arbitrary cooling rate ϕ. The kinetic crystallizability at unit cooling rate G can therefore be obtained

by normalizing G_ϕ with ϕ (i.e. $G = G_\phi/\phi$). It should be noted that this procedure was first realized by Jeziorny [20].

3. EXPERIMENTAL DETAILS

3.1. Materials

Syndiotactic polypropylene (sPP) used in this work was produced and supplied by AtoFina Petrochemicals (USA) based on a metallocene technology. Some physical properties of the resin, reported by the manufacturer, are density = 0.88 g/cm^3 (ASTM D1505), melt flow index = 2 g/10 min (ASTM D1238), tensile strength = 15 MPa (ASTM D638), tensile modulus = 480 MPa (ASTM D638), elongation at break = 11% (ASTM D790), flexural modulus = 340 MPa (ASTM D638), and notched Izod impact strength = 640 J/m (ASTM D256A).

Inorganic fillers used in this work are kaolin [$Al_2Si_2O_5(OH)_4$; Engelhard Corporation (USA)], talcum [$Mg_3Si_4O_{10}(OH)_2$, Pacific Commo Trading (Thailand)], marl [$CaSiO_3$; Pacific Commo Trading (Thailand)], titanium dioxide [TiO_2; Pacific Commo Trading (Thailand)], and SiO_2 [PPG Siam Silica (Thailand)]. Organic fillers are some sorbitol derivatives such as 1,3:2,4-dibenzylidene sorbitol [DBS; Ciba Specialty Chemicals (Switzerland)], 1,3:2,4-di-*p*-methyldibenzilidene sorbitol [MDBS; Ciba Specialty Chemicals (Switzerland)], and 1,3:2,4-di-*m*,*p*-methylbenzylidene sorbitol [DMDBS; Milliken Asia (Singapore)]. The average particle size of these fillers was measured by a Malvern Instruments Masterizer X particle size analyzer was found to be the followings (in descending order): marl = 42.5 ± 2.0 μm, SiO_2 = 36.4 ± 0.7 μm, DBS = 26.8 ± 1.0 μm, kaolin = 15.1 ± 1.5 μm, talc = 13.9 ± 1.8 μm, DMDBS = 6.7 ± 0.6 μm, TiO_2 = 5.3 ± 1.0 μm, and MDBS = 5.3 ± 0.6 μm.

3.2. Sample Preparation

All of the fillers used were first dried in a hot-air oven at 60°C for 14 hrs and then cooled down to room temperature. Each filler was then dry-mixed with sPP pellets in a tumble mixer for 10 min and later compounded in a Collin ZK25 self-wiping, co-rotating twin-screw extruder, operating at a screw speed of 50 rpm and

the die temperature of 190°C. Due to the limitation on the amount of sPP resin and fillers in possession, only 5 percent by weight (wt.%) of each inorganic filler or 1 wt.% of each organic filler was added to the sPP resin. A Planetrol 075D2 pelletizer was used to palletize the extrudate after coming out of the twin-screw kneader.

A film of each compound was prepared by melt-pressing sliced pellets between a pair of transparency films, which were sandwiched between a pair of stainless steel platens in a Wabash V50H compression press. The temperature of the platens was set at 190°C. The molding was pre-heated for 5 min, before compressing under an applied clamping force of 10 tons for another 5 min. Later, the film was cooled down, while still in the compression machine, until the temperature of the platens read 40°C. Each film specimen was subjected to thermal analysis.

3.3. Differential Scanning Calorimetry Measurements

Non-isothermal melt-crystallization and subsequent melting behavior of sPP samples filled with either an inorganic or an organic filler was investigated using a Perkin-Elmer Series 7 differential scanning calorimeter (DSC). Temperature calibration was carried out using a pure indium standard (T_m^0 = 156.6°C and ΔH_f^0 = 28.5 J/g) on every other run to ensure accuracy and reliability of the obtained data. To minimize thermal lag between the polymer sample and the furnace, each sample holder was loaded with a disc-shaped specimen, cut from the as-prepared film and weighed around 6.0 ± 0.5 mg. Each sample was used only once and all experimental runs were carried out under nitrogen atmosphere.

The experimental procedure started with heating each sample from 25°C at a rate of 80°C/min to 190°C in order to set a similar thermal history to each sample. To ensure complete melting, the sample was kept at 190°C for a holding period of 5 min, after which each sample was cooled at a desired rate ϕ, ranging from 2.5 to 20°C/min, to 30°C. The sample was then subjected to heating to observe the subsequent melting behavior (recorded using a heating rate of 20°C/min). Both non-isothermal melt-crystallization exotherms and subsequent melting endotherms were recorded for further analysis.

4. RESULTS AND DISCUSSION

4.1. Non-Isothermal Melt-Crystallization Behavior

Figure 1 shows non-isothermal melt-crystallization exotherms of neat sPP and sPP compounded with 1 wt.% of DMDBS and 5 wt.% of marl for six different cooling rates ranging from 2.5 to 20°C/min. In order to save some publishing space, the crystallization exothermic traces for other sample types were not shown. For most sample types, a single crystallization exotherm was visible. Only sPP samples compounded with kaolin, marl, and SiO_2 showed double crystallization exotherms. Since the temperature range where the high-temperature exotherm was observed was too high to be assign as the crystallization of the primary crystals formed during a cooling scan, only the low-temperature exotherm would be considered in this work. According to Figure 1, it is apparent that the exothermic trace for each type of sample became wider and shifted towards lower temperatures with increasing cooling rate used. Other sample types also exhibited a similar trend to what has been observed in Figure 1.

Figure 2 illustrates non-isothermal melt-crystallization exotherms, recorded at a cooling rate of 10°C/min, for all of the sample types investigated. Obviously, incorporation of these fillers, though with very small amount (i.e. 5 wt.% for inorganic fillers and 1 wt.% for organic fillers), was able to shift the crystallization exotherm towards a higher temperature than that of neat sPP. Among the exotherms shown (only the low-temperature exotherms for kaolin-filled, marl-filled, and SiO_2-filled sPP samples were considered), the non-isothermal crystallization exotherm of DBS-filled sPP sample was found to locate in the highest temperature range, followed by that of talc-filled, MDBS-filled, DMDBS-filled, kaolin-filled, SiO_2-filled, marl-filled, TiO_2-filled, and neat sPP samples, respectively. According to the results shown in Figure 2, it can be concluded based on the fillers used and the conditions studied in this work that DBS was the best, while TiO_2 was the worst, nucleating agent for sPP.

In order to quantify the non-isothermal melt-crystallization data obtained, some characteristic parameters are defined, viz. $T_{0.01}$ = the temperature at 1% relative crystallinity, T_p = the temperature at the maximum crystallization rate or the peak

temperature, and $T_{0.99}$ = the temperature at 99% relative crystallinity. $T_{0.01}$ and $T_{0.99}$ are used here to represent the beginning and the ending of the non-isothermal crystallization process. Table 1 summarizes $T_{0.01}$, T_p, and $T_{0.99}$ values for all of the sample types studied. For a given sample type, all of the $T_{0.01}$, T_p, and $T_{0.99}$ values were found to shift to lower values with increasing cooling rate. The results imply that the higher cooling rate, the slower the crystallization process began and ended (based on the temperature domain).

In order to compare the nucleation ability among the fillers studied in a quantitative manner, some characteristic parameters are, again, defined, viz. $\Delta T_{0.01}$ = the difference between the $T_{0.01}$ values of an sPP compound and the neat sPP and ΔT_p = the difference between the T_p values of an sPP compound and the neat sPP. The average $\Delta T_{0.01}$ and ΔT_p values (calculated for a particular sample type from all of the six cooling rates studied) for all of the sPP compounds investigated are as follows: for DSB-filled sPP, they are 17.7 ± 1.3 and 17.8 ± 1.3°C; for MDBS-filled sPP, they are 15.5 ± 1.8 and 16.1 ± 1.7°C; for DMDBS-filled sPP, they are 11.6 ± 0.9 and 14.8 ± 1.0°C; for kaolin-filled sPP, they are 12.4 ± 1.3 and 13.6 ± 1.6°C; for talc-filled sPP, they are 16.2 ± 1.1 and 16.6 ± 0.8°C; for marl-filled sPP, they are 9.2 ± 0.8 and 11.6 ± 1.4°C; for TiO_2-filled sPP, they are 5.5 ± 1.3 and 8.9 ± 0.9°C; and for SiO_2-filled sPP, they are 12.5 ± 1.2 and 13.7 ± 1.7°C. Based on these values, the nucleation ability among these fillers can be ranked from best to worst as follows: DBS > talcum > MDBS > SiO_2 ~ kaolin ~ DMDBS > marl > TiO_2.

After non-isothermal melt-crystallization, each sample was immediately subjected to heating at a heating rate of 20°C/min to 180°C in order to observe the subsequent melting behavior. Figure 3 illustrates subsequent melting endotherms of neat sPP and sPP compounded with 1 wt.% of DMDBS and 5 wt.% of marl after non-isothermal melt-crystallization for six different cooling rates ranging from 2.5 to 20°C/min. In order to save some publishing space, the melting endothermic traces for other sample types were not shown. Clearly, almost all of the resulting endotherms exhibited double melting peaks, with size and sharpness being dependent on the cooling rate studied and on the type of filler used. Qualitatively, the low-temperature melting peak was generally found to increase in its sizes and sharpness

and move toward a higher temperature with a decrease in the cooling rate used. On the contrary, the high-temperature melting peak generally became smaller with decreasing cooling rate and, for most of the filled systems investigated (with an exception to TiO_2-filled system), it even disappeared altogether when the cooling rate used was lower than 5°C/min. These observations should be a direct result of the increased stability of the primary crystallites formed during cooling at slow cooling rates [21].

Let us carefully consider Figures 3 and 4, it is only in case of marl that triple melting peaks were observed for cooling rates greater than or equal to 5°C/min. Since we observed the subsequent melting behavior using a fixed heating rate 20°C/min, it is very interesting to see whether the triple melting peaks can be observed at other heating rates. In so doing, a separate experiment was carried out in which marl-filled sPP samples were non-isothermally crystallized at a fixed cooling rate of 15°C/min and the subsequent melting behavior was observed using various heating rates ranging from 5 to 30°C/min. It was found that the triple melting peaks were clearly visible in all of the subsequent heating thermograms obtained and any change in the heating rate used did not affect the position of the three peaks. It, however, affected the breadth and height of those peaks. At this point, the origin of the triple melting behavior in marl-filled sPP samples was not known and it should be a subject for further investigation.

4.2. Avrami Analysis

In order to obtain the relevant kinetic information for the non-isothermal melt-crystallization behavior of all the samples investigated, the raw data such as those shown in Figure 1 need to be converted into relative crystallinity functions of temperature $\theta(T)$ or of time $\theta(t)$, depending on the macrokinetic model used to analyze the data. The conversion from the raw data into $\theta(T)$ functions can be done according to Equation (2) and the conversion from $\theta(T)$ functions into $\theta(t)$ functions can be carried by transforming the temperature scale into the time scale according to Equation (3). Converted $\theta(T)$ and $\theta(t)$ functions for neat sPP and sPP compounded with 1 wt.% of DMDBS and 5 wt.% of marl after non-isothermal melt-crystallization

for six different cooling rates ranging from 2.5 to 20°C/min are shown in Figures 5 and 6, respectively.

An important kinetic parameter which can be taken directly from a $\theta(t)$ function is the half-time of crystallization $t_{0.5}$, which is defined as the time interval from the onset of crystallization to the time at which the crystallization process is half completed. The $t_{0.5}$ values for all of the sample types and cooling conditions studied are summarized in Table 2. Obviously, the $t_{0.5}$ value for each sample type was found to increase with decreasing cooling rate, while its inversed value, i.e. the reciprocal half-time of crystallization $t_{0.5}^{-1}$ (also summarized in Table 2), was found to increase with increasing cooling rate, suggesting slow crystallization rates at low cooling rates.

Analysis of the experimental data can be carried out by directly fitting Equation (1) to the $\theta(t)$ functions, such as those shown in Figure 6. In the fitting, only the relative crystallinity data in the range of 10 to 80% were used. The obtained values of the Avrami kinetic parameters (i.e. n_a and K_a) along with the r^2 parameter, signifying the quality of the fitting, for all of the sample types and cooling conditions studied are summarized in Table 2.

For all of the sample types studied, the Avrami exponent n_a was found to vary between ca. 2.9 to 6.8. Specifically, for neat sPP, n_a was found to vary between ca. 3.1 to 6.8, which is in good agreement with the values of ca. 2.4 to 5.3 found in an earlier work [11]. For all of the sPP compounds, n_a was found to vary between ca. 2.9 to 4.3. The Avrami crystallization rate constant K_a for a given sample type was found to increase with increasing cooling rate, which is in a similar manner to that of $t_{0.5}^{-1}$. In fact, for any given sample type and cooling rate studied, the values of both K_a and $t_{0.5}^{-1}$ are very comparable (see Table 2). According to the results shown in Table 2, addition of these fillers accelerated crystallization, as reflected by the reduction in both K_a and $t_{0.5}^{-1}$ values of sPP compounds in comparison with those of neat sPP.

4.3. Ziabicki's Kinetic Crystallizability Analysis

Table 3 summarizes the values of $T_{max,\phi}$, $\dot{\theta}_{max,\phi}$, and D_ϕ for neat sPP and sPP filled with various inorganic and organic fillers. The values of $\dot{\theta}_{max,\phi}$ and D_ϕ were used to calculate the Ziabicki's kinetic crystallizability G, the values of which are also summarized in Table 3. For a given sample type, the temperature at the maximum crystallization rate $T_{max,\phi}$ was found to decrease with increasing cooling rate in a similar manner to the peak temperature T_p summarized in Table 1, while both of the maximum crystallization rate $\dot{\theta}_{max,\phi}$ and the width at half-height of the derivative relative crystallinity function of temperature D_ϕ were all found to increase with increasing cooling rate. Based on these values, the resulting cooling rate-dependent kinetic crystallizability G_ϕ (results not shown) was an increasing function of the cooling rate, and, after normalizing with the corresponding cooling rate, the kinetic crystallizability G for a given sample type can be calculated and the G values for all of the sample types and the cooling rates studied are summarized in Table 3.

The practical meaning of G is the ability of a semi-crystalline polymer to crystallize when it is cooled from the melt to the glassy state at a unit cooling rate, hence the higher the G value is, the more readily the polymer can crystallize. According to Table 3, the average G value for neat sPP was found to be 0.90, while the average G values for all of the sPP compounds ranged between 0.93 and 1.00, which were all greater than that of neat sPP, suggesting that the sPP compounds were more likely to crystallize than the neat sPP. However, since the average G values for all the sPP compounds were quite close to one another, it was not possible to use the average G values obtained to rank the nucleation ability among the fillers studied.

5. CONCLUSIONS

The kinetics of non-isothermal melt-crystallization of syndiotactic polypropylene (sPP) compounded with 5 percent by weight (wt.%) of some inorganic fillers [i.e. kaolin, talcum, marl, titanium dioxide (TiO_2), and silicon dioxide (SiO_2)] and 1 wt.% of some organic fillers, which are some sorbital derivatives (i.e. DBS, MDBS, and DMDBS) was investigated and reported for the first time. The non-isothermal melt-crystallization trace for each sample type

became wider and shifted towards lower temperatures with increasing cooling rate used. Comparison among the non-isothermal melt-crystallization traces for all of the sample types investigated at a fixed cooling rate of 10°C/min revealed that DBS was the best, while TiO_2 was the worst, nucleating agent for sPP. Careful analysis of the onset temperature shift (i.e. $\Delta T_{0.01}$) suggested the ability for these fillers to nucleate sPP in the following order: DBS > talcum > MDBS > SiO_2 ~ kaolin ~ DMDBS > marl > TiO_2, with DBS being able to shift the crystallization exotherm by ca. 18°C on average, while TiO_2 being able to shift the crystallization exotherm by only ca. 6°C on average, from that of neat sPP. The Avrami analysis revealed the Avrami exponent for sPP compounds being in the range of 2.9 to 4.3, with the values for neat sPP being in the range of 3.1 to 6.8. Lastly, the Ziabicki's crystallizability of sPP compounds was found to range between 0.93 and 1.00 which was greater than that of neat sPP, suggesting the enhancement in the crystallization ability of sPP with addition of these fillers.

ACKNOWLEDGMENTS

The authors acknowledge partial supports received from the Petroleum and Petrochemical Technology Consortium (through a Thai governmental loan from the Asian Development Bank), Chulalongkorn University (through a grant from the Ratchadapisek Somphot Endowment Fund for the foundation of the Conductive and Electroactive Polymers Research Unit), and the Petroleum and Petrochemical College, Chulalongkorn University.

REFERENCES

[1] Ewen J.A., Johns R.L., Razavi A., and Ferrara J.D., J Am Chem Soc 1988, 110, 6255.

[2] Natta G., Pasquon I., and Zambelli A., J Am Chem Soc 1962, 84, 1488.

[3] Rodriguez-Arnold J., Bu Z., and Cheng S.Z.D., J Macromol Sci-Rev Macromol Chem Phys 1995, C35, 117.

[4] Schardi J., Sun L., Kimura S., and Sugimoto R., J Plastic Film Sheeting 1996, 12, 157.

[5] Sun L., Shamshoum E., and Dekunder G., SPE-ANTEC Proc 1996, 1965.

[6] Gownder M., SPE-ANTEC Proc 1998, 1511.

[7] Sura R.K., Desai P., and Abhiraman A.S., SPE-ANTEC Proc 1999, 1764.

[8] Guadagno L., Naddeo C., D'Aniello C., Maio L., Vitoria V., and Acierno D., Macromol Symp 2002, 180, 23.

[9] Loos J., Bonnet M., and Petermann J., Polymer 2000, 41, 351.

[10] Supaphol P. and Spruiell J.E., J Appl Polym Sci 2000, 75, 44.

[11] Supaphol P., J Appl Polym Sci 2000, 78, 338.

[12] Supaphol P. and Spruiell J.E., SPE-ANTEC Proc 1999, 1834.

[13] Avrami M., J Chem Phys 1939, 7, 1103.

[14] Avrami M., J Chem Phys 1940, 8, 212.

[15] Avrami M., J Chem Phys 1941, 9, 177.

[16] Wunderlich B., Macromolecular Physics, vol. 2, Academic Press, New York, 1976, 147.

[17] Ziabicki A., Appl Polym Symp 1967, 6, 1.

[18] Ziabicki A., Polymer 1967, 12, 405.

[19] Ziabicki A., Fundamental of Fiber Spinning, Wiley, New York, 1976, 112-114.

[20] Jeziorny A., Polymer 1978, 19, 1142.

[21] Supaphol P., J Appl Polym Sci 2001, 82, 1083.

CAPTION OF TABLES

CAPTION OF FIGURES

Figure 1 Non-isothermal melt-crystallization exotherms of (a) neat sPP and sPP compounded with (b) 1 percent by weight of DMDBS and (c) 5 percent by weight of marl for six different cooling rates ranging from 2.5 to 20°C/min.

Figure 2 Non-isothermal melt-crystallization exotherms of neat sPP and all of the sPP compounds for a fixed cooling rate of 10°C/min.

Figure 3 Subsequent melting endotherms of (a) neat sPP and sPP compounded with (b) 1 percent by weight of DMDBS and (c) 5 percent by weight of marl after non-isothermal melt-crystallization for six different cooling rates ranging from 2.5 to 20°C/min.

Figure 4. Subsequent melting endotherms (recorded at a fixed heating rate of 20°C/min) of neat sPP and all of the sPP compounds after non-isothermal melt-crystallization for a fixed cooling rate of 10°C/min.

Figure 5. Relative crystallinity as a function of temperature of (a) neat sPP and sPP compounded with (b) 1 percent by weight of DMDBS and (c) 5 percent by weight of marl for six different cooling rates: (●) 2.5, (○) 5, (■) 7.5, (□) 10, (▲) 15, and (△) 20°C/min.

Figure 6. Relative crystallinity as a function of time of (a) neat sPP and sPP compounded with (b) 1 percent by weight of DMDBS and (c) 5 percent by weight of marl for six different cooling rates: (●) 2.5, (○) 5, (■) 7.5, (□) 10, (▲) 15, and (△) 20°C/min. The raw data are shown as various geometrical points, while the Avrami predictions are shown as solid lines.

Table 1. Characteristic data for non-isothermal melt-crystallization exotherms of neat sPP and sPP compounds

ϕ	neat sPP			DBS-filled sPP			MDBS-filled sPP		
(°C min^{-1})	$T_{0.01}$ (°C)	T_p (°C)	$T_{0.99}$ (°C)	$T_{0.01}$ (°C)	T_p (°C)	$T_{0.99}$ (°C)	$T_{0.01}$ (°C)	T_p (°C)	$T_{0.99}$ (°C)
2.5	84.0	77.6	72.7	101.3	92.9	87.1	96.6	90.7	85.8
5	82.6	71.9	66.1	99.9	90.5	82.6	98.5	89.0	81.7
7.5	79.8	67.5	61.1	95.7	85.2	74.8	94.3	83.6	73.5
10	76.0	64.1	58.4	94.0	82.7	72.2	91.2	80.9	68.6
15	72.1	60.0	53.6	89.9	78.1	68.1	89.5	77.9	66.6
20	68.8	57.9	49.7	88.7	76.4	63.2	85.8	73.7	62.6

ϕ	DMDBS-filled sPP			kaolin-filled sPP			talc-filled sPP		
(°C min^{-1})	$T_{0.01}$ (°C)	T_p (°C)	$T_{0.99}$ (°C)	$T_{0.01}$ (°C)	T_p (°C)	$T_{0.99}$ (°C)	$T_{0.01}$ (°C)	T_p (°C)	$T_{0.99}$ (°C)
2.5	95.9	90.9	86.2	96.8	90.2	85.5	101.7	93.6	86.7
5	93.0	86.4	80.1	95.4	86.1	78.5	97.7	87.8	78.5
7.5	90.5	82.2	74.7	92.1	81.8	74.6	94.7	84.5	75.2
10	88.1	80.0	72.4	90.5	79.9	71.4	91.8	81.7	72.7
15	83.7	75.9	67.7	82.7	73.7	64.3	88.8	77.2	66.3
20	81.6	72.5	63.2	80.0	69.0	58.8	85.5	74.0	61.1

ϕ	marl-filled sPP			TiO_2-filled sPP			SiO_2-filled sPP		
(°C min^{-1})	$T_{0.01}$ (°C)	T_p (°C)	$T_{0.99}$ (°C)	$T_{0.01}$ (°C)	T_p (°C)	$T_{0.99}$ (°C)	$T_{0.01}$ (°C)	T_p (°C)	$T_{0.99}$ (°C)
2.5	93.6	88.5	84.9	91.7	86.9	81.8	97.7	90.2	85.9
5	91.1	82.9	77.2	86.8	80.9	75.3	94.9	86.2	79.9
7.5	88.8	80.4	73.6	83.0	76.6	70.3	93.3	82.8	74.3
10	84.3	76.9	69.7	81.9	73.6	66.5	88.1	80.0	72.4
15	82.5	72.5	63.8	78.1	69.3	61.8	82.6	72.1	63.4
20	78.4	67.2	58.2	74.5	65.0	56.3	81.5	69.9	59.7

Table 2. Non-isothermal melt-crystallization kinetic parameters for neat sPP and sPP compounds based on Avrami analysis

	neat sPP					DBS-filled sPP					MDBS-filled sPP				
ϕ	n_a	K_a	r^2	$t_{0.5}$	$t_{0.5}^{-1}$	n_a	K_a	r^2	$t_{0.5}$	$t_{0.5}^{-1}$	n_a	K_a	r^2	$t_{0.5}$	$t_{0.5}^{-1}$
($^{\circ}$C min^{-1})		(min^{-1})		(min)	(min^{-1})		(min^{-1})		(min)	(min^{-1})		(min^{-1})		(min)	(min^{-1})
2.5	3.86	0.20	0.9989	4.59	0.22	3.36	0.22	0.9989	4.07	0.25	4.09	0.24	0.9998	3.79	0.26
5	3.08	0.36	0.9944	2.47	0.41	3.04	0.38	0.9992	2.33	0.43	3.83	0.37	0.9994	2.49	0.40
7.5	3.51	0.48	0.9943	1.91	0.52	3.36	0.49	0.9999	1.82	0.55	3.78	0.49	0.9998	1.88	0.53
10	4.68	0.59	0.9964	1.99	0.50	3.20	0.63	0.9997	1.43	0.70	3.87	0.65	0.9994	1.42	0.70
15	6.17	0.71	0.9981	1.34	0.75	3.83	0.87	0.9997	1.05	0.96	3.89	0.92	0.9997	0.99	1.01
20	6.79	1.03	0.9995	0.77	1.30	3.02	1.22	0.9998	0.73	1.37	4.12	1.12	0.9998	0.81	1.23
	DMDBS-filled sPP					kaolin-filled sPP					talc-filled sPP				
ϕ	n_a	K_a	r^2	$t_{0.5}$	$t_{0.5}^{-1}$	n_a	K_a	r^2	$t_{0.5}$	$t_{0.5}^{-1}$	n_a	K_a	r^2	$t_{0.5}$	$t_{0.5}^{-1}$
($^{\circ}$C min^{-1})		(min^{-1})		(min)	(min^{-1})		(min^{-1})		(min)	(min^{-1})		(min^{-1})		(min)	(min^{-1})
2.5	3.06	0.36	0.9999	2.46	0.41	3.52	0.27	0.9994	3.35	0.30	2.88	0.23	0.9993	3.89	0.26
5	3.57	0.54	0.9998	1.69	0.59	3.29	0.41	0.9993	2.30	0.44	3.38	0.37	0.9996	2.43	0.41
7.5	3.81	0.63	0.9999	1.45	0.69	3.62	0.53	0.9993	1.73	0.58	3.45	0.53	0.9998	1.71	0.59
10	3.92	0.87	0.9997	1.05	0.95	3.55	0.69	0.9995	1.32	0.76	3.59	0.72	0.9997	1.26	0.80
15	3.89	1.17	0.9998	0.77	1.30	3.65	1.11	0.9999	7.75	0.13	4.08	0.92	0.9996	0.99	1.01
20	3.79	1.50	0.9997	0.60	1.66	4.01	1.26	0.9998	0.73	1.37	4.22	1.14	0.9992	0.80	1.25
	marl-filled sPP					TiO_2-filled sPP					SiO_2-filled sPP				
ϕ	n_a	K_a	r^2	$t_{0.5}$	$t_{0.5}^{-1}$	n_a	K_a	r^2	$t_{0.5}$	$t_{0.5}^{-1}$	n_a	K_a	r^2	$t_{0.5}$	$t_{0.5}^{-1}$
($^{\circ}$C min^{-1})		(min^{-1})		(min)	(min^{-1})		(min^{-1})		(min)	(min^{-1})		(min^{-1})		(min)	(min^{-1})
2.5	3.65	0.35	0.9997	2.81	0.36	3.42	0.36	0.9999	2.47	0.40	3.98	0.23	0.9988	3.92	0.26
5	4.25	0.43	0.9997	2.24	0.45	3.71	0.58	0.9999	1.56	0.64	3.66	0.41	0.9995	2.22	0.45
7.5	3.95	0.63	0.9998	1.46	0.68	3.77	0.74	0.9999	1.07	0.93	3.25	0.53	0.9991	1.70	0.59
10	3.11	0.92	0.9998	0.97	1.03	3.92	0.83	0.9999	1.10	0.91	3.51	0.64	0.9999	1.40	0.71
15	3.35	1.09	0.9997	0.83	1.21	3.95	1.13	0.9999	0.81	1.24	3.22	1.01	0.9994	0.89	1.13
20	3.26	1.69	0.9999	0.53	1.89	4.13	1.36	0.9999	0.67	1.49	2.87	1.30	0.9989	0.68	1.47

Table 3. Non-isothermal melt-crystallization kinetic parameters for neat sPP and sPP compounds based on Ziabicki's crystallizability analysis

ϕ	neat sPP				DBS-filled sPP				MDBS-filled sPP			
(oC min-1)	T_{max_ϕ} (°C)	θ_{max_ϕ} (min^{-1})	D_ϕ	G	T_{max_ϕ} (°C)	θ_{max_ϕ} (min^{-1})	D_ϕ	G	T_{max_ϕ} (°C)	θ_{max_ϕ} (min^{-1})	D_ϕ	G
2.5	76.2	0.324	7.89	1.09	92.2	0.309	7.45	0.98	90.5	0.384	6.08	0.99
5	70.0	0.609	7.53	0.98	89.5	0.472	10.35	1.04	88.2	0.594	7.14	0.90
7.5	65.5	0.917	6.58	0.86	86.0	0.666	10.54	0.99	83.0	0.730	9.10	0.94
10	63.2	1.606	4.48	0.77	82.0	0.833	11.34	1.01	80.7	0.993	8.28	0.88
15	59.2	2.221	5.18	0.82	78.0	1.310	10.13	0.94	77.7	1.395	9.37	0.93
20	57.7	2.699	6.16	0.88	76.3	1.461	12.59	0.98	73.3	1.801	9.81	0.94
Average				0.90				0.99				0.93

ϕ	DMDBS-filled sPP				kaolin-filled sPP				talc-filled sPP			
(oC min-1)	T_{max_ϕ} (°C)	θ_{max_ϕ} (min^{-1})	D_ϕ	G	T_{max_ϕ} (°C)	θ_{max_ϕ} (min^{-1})	D_ϕ	G	T_{max_ϕ} (°C)	θ_{max_ϕ} (min^{-1})	D_ϕ	G
2.5	91.0	0.438	5.45	1.02	89.7	0.382	6.18	1.00	93.0	0.268	9.16	1.05
5	86.2	0.758	5.87	0.95	85.7	0.573	8.14	0.99	87.2	0.510	8.20	0.89
7.5	82.0	0.947	7.17	0.96	81.0	0.773	9.22	1.01	84.0	0.713	9.51	0.96
10	80.0	1.309	6.80	0.95	79.2	0.979	9.17	0.96	81.5	1.032	8.47	0.93
15	76.0	1.816	7.46	0.96	73.5	1.560	8.78	0.97	77.2	1.461	8.94	0.93
20	72.7	2.196	8.10	0.95	68.3	1.952	9.15	0.95	74.0	1.845	9.32	0.91
Average				0.96				0.98				0.94

ϕ	marl-filled sPP				TiO_2-filled sPP				SiO_2-filled sPP			
(oC min-1)	T_{max_ϕ} (°C)	θ_{max_ϕ} (min^{-1})	D_ϕ	G	T_{max_ϕ} (°C)	θ_{max_ϕ} (min^{-1})	D_ϕ	G	T_{max_ϕ} (°C)	θ_{max_ϕ} (min^{-1})	D_ϕ	G
2.5	88.2	0.492	4.88	1.02	86.7	0.484	4.55	0.94	89.5	0.384	6.14	1.00
5	82.2	0.737	6.26	0.98	80.7	0.852	5.32	0.96	85.7	0.626	7.49	1.00
7.5	80.0	0.953	7.13	0.96	76.5	1.078	6.49	0.99	82.0	0.737	9.64	1.01
10	76.5	1.128	8.61	1.03	73.2	1.262	7.24	0.97	78.2	0.869	10.51	0.97
15	71.7	1.440	9.72	0.99	68.7	1.721	8.10	0.99	71.0	1.319	10.92	1.02
20	66.7	2.031	8.83	0.95	64.7	2.154	8.47	0.97	68.3	1.586	12.07	1.02
Average				0.99				0.97				1.00

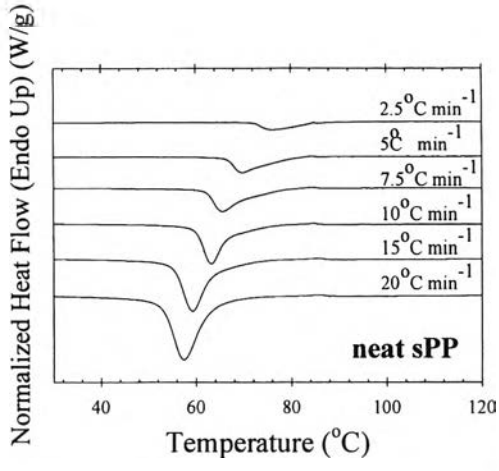
Normalized Heat Flow (Endo Up) (W/g)
2.5°C min-1
5°C min-1
7.5°C min-1
10°C min-1
15°C min-1
20°C min-1
neat sPP
40
60
80
100
120
Temperature (°C)

(a)

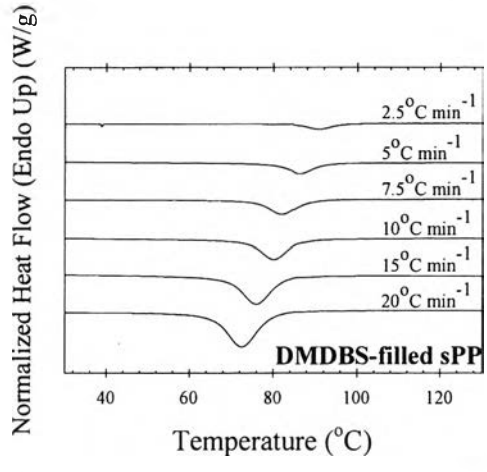
Normalized Heat Flow (Endo Up) (W/g)
2.5°C min-1
5°C min-1
7.5°C min-1
10°C min-1
15°C min-1
20°C min-1
DMDBS-filled sPP
40
60
80
100
120
Temperature (°C)

(b)

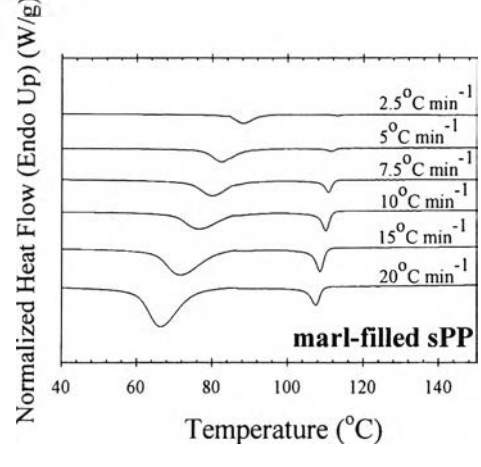
Normalized Heat Flow (Endo Up) (W/g)
2.5°C min-1
5°C min-1
7.5°C min-1
10°C min-1
15°C min-1
20°C min-1
marl-filled sPP
40
60
80
100
120
140
Temperature (°C)

(c)

Figure 1

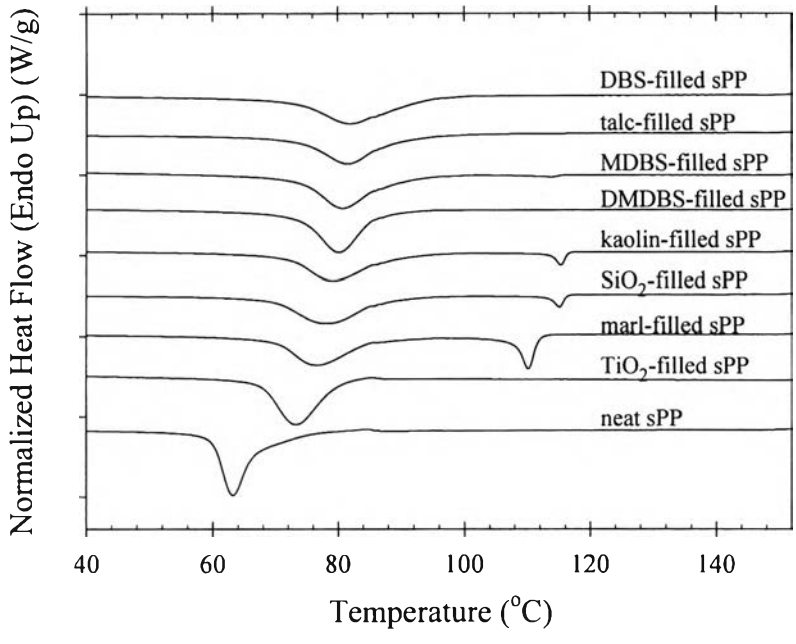
Normalized Heat Flow (Endo Up) (W/g)
DBS-filled sPP
talc-filled sPP
MDBS-filled sPP
DMDBS-filled sPP
kaolin-filled sPP
SiO2-filled sPP
marl-filled sPP
TiO2-filled sPP
neat sPP
40
60
80
100
120
140
Temperature (°C)

Figure 2

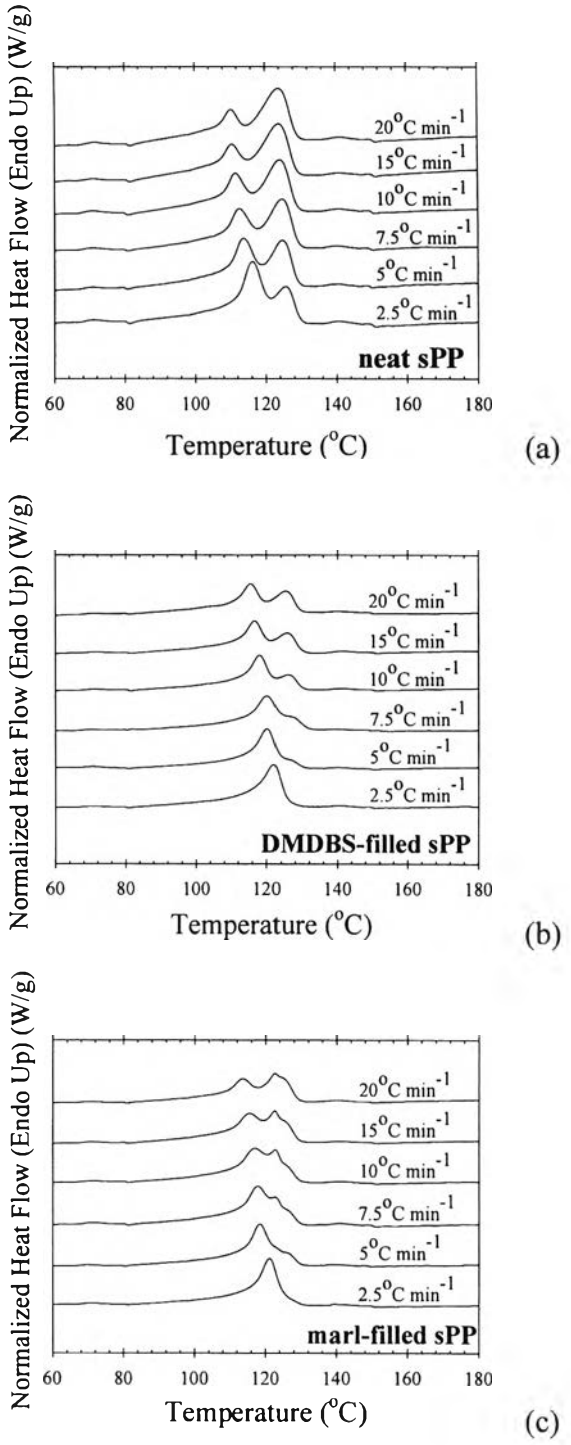
Normalized Heat Flow (Endo Up) (W/g)
20°C min-1
15°C min-1
10°C min-1
7.5°C min-1
5°C min-1
2.5°C min-1
neat sPP
60 80 100 120 140 160 180
Temperature (°C)
(a)
Normalized Heat Flow (Endo Up) (W/g)
20°C min-1
15°C min-1
10°C min-1
7.5°C min-1
5°C min-1
2.5°C min-1
DMDBS-filled sPP
60 80 100 120 140 160 180
Temperature (°C)
(b)
Normalized Heat Flow (Endo Up) (W/g)
20°C min-1
15°C min-1
10°C min-1
7.5°C min-1
5°C min-1
2.5°C min-1
marl-filled sPP
60 80 100 120 140 160 180
Temperature (°C)
(c)

Figure 3

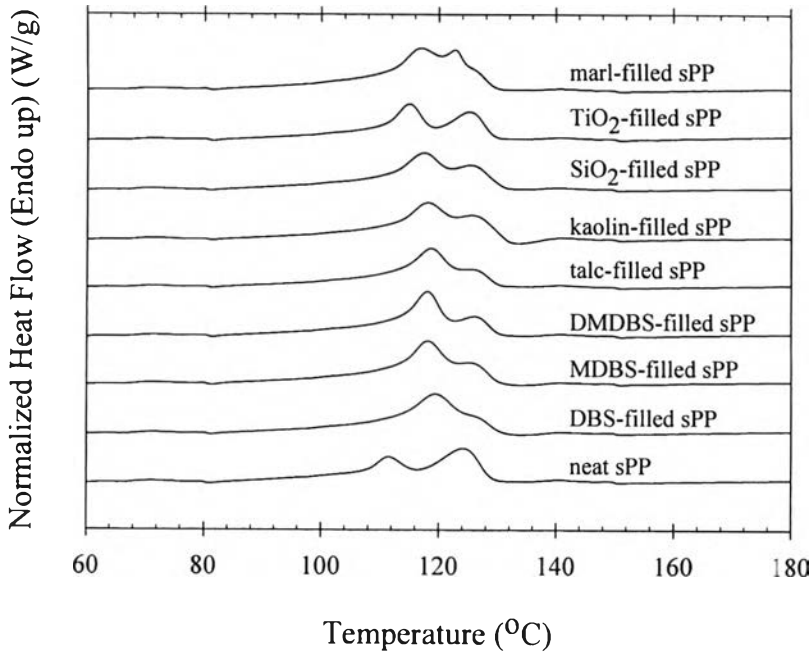
Normalized Heat Flow (Endo up) (W/g)
marl-filled sPP
TiO2-filled sPP
SiO2-filled sPP
kaolin-filled sPP
talc-filled sPP
DMDBS-filled sPP
MDBS-filled sPP
DBS-filled sPP
neat sPP
60
80
100
120
140
160
180
Temperature (°C)

Figure 4

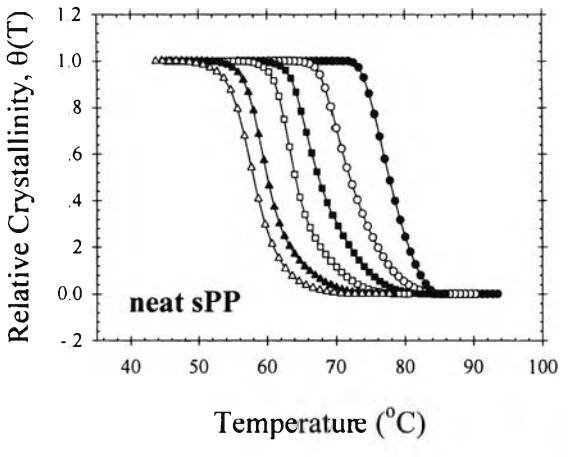
Relative Crystallinity, θ(T)
1.2
1.0
.8
.6
.4
.2
0.0
-.2
neat sPP
40
50
60
70
80
90
100
Temperature (°C)

(a)

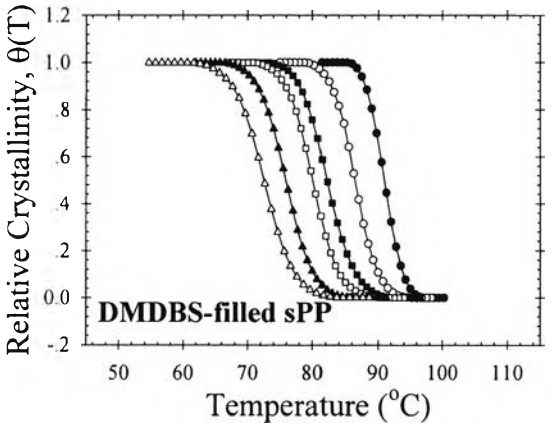
Relative Crystallinity, θ(T)
1.2
1.0
.8
.6
.4
.2
0.0
-.2
DMDBS-filled sPP
50
60
70
80
90
100
110
Temperature (°C)

(b)

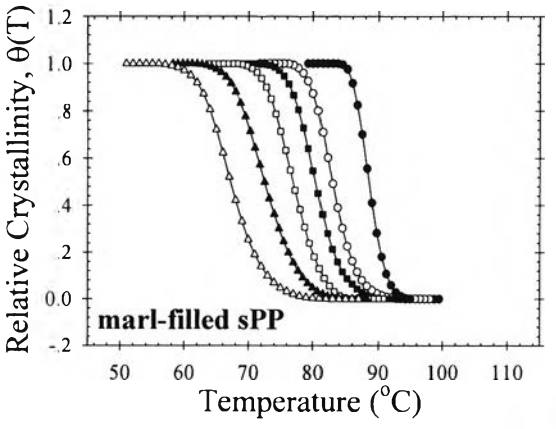
Relative Crystallinity, θ(T)
1.2
1.0
.8
.6
.4
.2
0.0
-.2
marl-filled sPP
50
60
70
80
90
100
110
Temperature (°C)

(c)

Figure 5

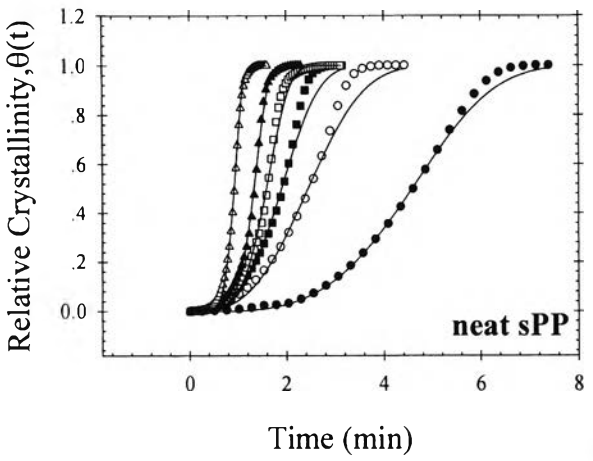
Relative Crystallinity,θ(t)
1.2
1.0
.8
.6
.4
.2
0.0
neat sPP
0
2
4
6
8
Time (min)

(a)

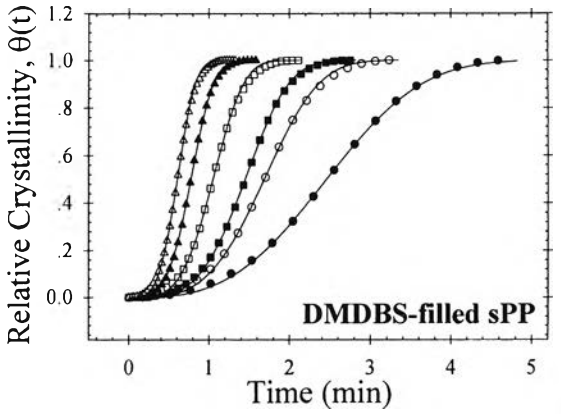
Relative Crystallinity, θ(t)
1.2
1.0
.8
.6
.4
.2
0.0
DMDBS-filled sPP
0
1
2
3
4
5
Time (min)

(b)

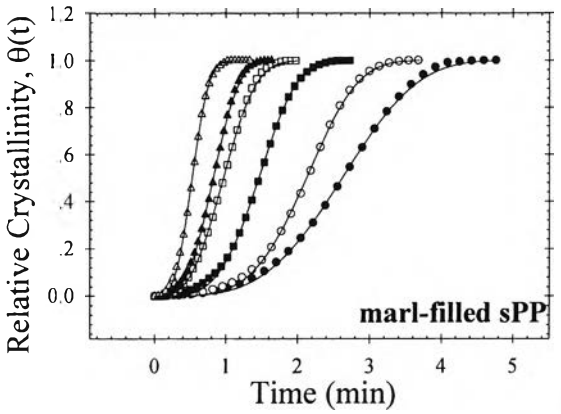
Relative Crystallinity, θ(t)
1.2
1.0
.8
.6
.4
.2
0.0
marl-filled sPP
0
1
2
3
4
5
Time (min)

(c)

Figure 6